J Mater Sci (2008) 43:5942–5947
DOI 10.1007/s10853-008-2862-0

Effects of rolling and hot pressing on mechanical properties of boron carbide-based ceramics

Nina Orlovskaya · Sergey Yarmolenko · Jag Sankar · Jakob Kuebler · Mykola Lugovy

Received: 25 July 2007 / Accepted: 3 July 2008 / Published online: 27 July 2008

Abstract A study of hot pressed B_4C-based laminates, after rolling and without rolling, has been performed to elucidate the existence of fracture resistance/crack length anisotropy induced by this processing technique. While the crack lengths/fracture resistance was affected significantly by the presence of the residual stresses in $B_4C/B_4C–ZrB_2$ laminates, no differences in Vickers crack lengths were observed in B_4C/B_4C laminates prepared by rolling and hot pressing, as compared to the crack lengths seen in pure B_4C ceramics prepared by hot pressing without rolling. X-ray diffraction analysis confirmed that no texture has been formed during the rolling and hot pressing of B_4C ceramics.

Introduction

Ceramics offer a number of attractive properties, including high specific stiffness, high specific strength, low thermal conductivities, and chemical inertness in many environments. Ceramics and ceramic composites are attractive materials for use in armor systems due to low density, superior hardness, and high compressive strength values relative to metals [1–3]. Ceramic laminates with strong interfaces, combined with excellent fracture toughness and damage tolerance, can potentially provide an even better ballistic performance than traditional single phase ceramics or particulate ceramic composites.

One of the most important lightweight body armor materials is boron carbide-based ceramic composites [4, 5 Polycrystalline B_4C ceramics have high hardness in the range of 32–35 GPa [6–8], a high Young's modulus in the range of 430–450 GPa [9], and a bending strength in the range of 400–600 MPa [10]. Room temperature isotropic elastic moduli of B_4C show that its bulk, shear and Young's moduli are substantially higher than those of most solids. Consequently, B_4C belongs to the so-called strong solids classification. Conversely, B_4C ceramics have a relatively low fracture toughness of 2.8–3.3 MPa $m^{1/2}$ [11]. There is a possibility of a significant increase in the apparent fracture toughness (up to 8.2 MPa $m^{1/2}$ or higher) via design of residual stresses in multilayered B_4C-based composites [12, 13]. Non-linear stress–strain behavior of B_4C/ B_4C laminates with weak interfaces was reported earlier in [14]. A decrease in brittleness has great potential for the realization of improved armor material systems.

It was recently reported that B_4C single crystals exhibit a strong anisotropy of the elastic constants [15]. The elastic constants for B_4C single crystals were determined in the coordinate system where x_1 was parallel to $[10\bar{1}0]$ crystallographic direction, x_2 was parallel to $[\bar{1}2\bar{1}0]$ crystallographic direction, and x_3 was parallel to [0001] crystallographic direction. The reported values of room temperature elastic constants for B_4C single crystals are $c_{11} = 542.81$, $c_{33} = 534.54$, $c_{13} = 63.51$, $c_{12} = 130.59$, and $c_{44} = 164.79$ GPa. Accordingly, the maximum ratio of elastic constants c_{11} and c_{13} is equal to 8.55. Based on the

N. Orlovskaya (✉)
University of Central Florida, Orlando, FL, USA
e-mail: norlovsk@mail.ucf.edu; nil2903@gmail.com

S. Yarmolenko · J. Sankar
North Carolina A&T State University, Greensboro, NC, USA

J. Kuebler
Material Science and Technology, EMPA, Duebendorf, Switzerland

M. Lugovy
Institute for Problems of Materials Science, Kyiv, Ukraine

analysis of Cauchy's relationships, Poisson's ratios, and elastic anisotropic factors for the single crystal elastic constants, it was concluded that B_4C is more anisotropic in elasticity and interatomic bonding than most solids. Anisotropy of elastic properties, if detected, should result in differences in the mechanical properties of boron carbide ceramics and can significantly affect the ballistic performance of the material. The ballistic performance depends on the hardness and elastic modulus of the material, therefore materials with low elastic modulus will underperform relative to the materials with high elastic modulus. In this way anisotropy can significantly affect the ballistic performance and other mechanical properties.

It is important to know if anisotropy can be introduced into the polycrystalline B_4C composites via different manufacturing procedures, such as rolling or hot pressing. It was reported that rolling and hot pressing induced texture in Si_3N_4 laminates, which resulted in anisotropy in the fracture toughness values [16]. It is known that the contact pressure in the deformation zone during rolling can be very high; therefore, the texturing of the polycrystalline B_4C can occur during rolling. If texturing occurs with the preferential alignment in the direction, which has the lowest c_{13} elastic constant, it will dramatically affect both ballistic performance and fracture toughness of the material.

The goal of the present research is to determine if there is any anisotropy in the fracture resistance of B_4C ceramics introduced during manufacturing processes such as rolling and hot pressing. To achieve this goal, both hot pressed B_4C ceramics without rolling and B_4C/B_4C laminates prepared by rolling and hot pressing without thermal residual stresses were investigated. For comparison B_4C/B_4C–30 wt%ZrB_2 with thermal residual stress and B_4C–30 wt%SiC/B_4C–30 wt%SiC laminates without thermal residual stresses have been also tested.

Experimental

Three types of the laminates, (1) B_4C/B_4C, (2) B_4C–30 wt%SiC/B_4C–30 wt%SiC, and (3) B_4C/B_4C–30 wt% ZrB_2, have been produced using the techniques described in detail elsewhere [17]. In the case of the first two compositions, all layers have been prepared with the same composition. For the first laminate, it is pure B_4C composition, for the second laminate it is B_4C–30 wt%SiC composition. In the case of the third laminate the layers were made using two compositions—pure B_4C and B_4C–30 wt%ZrB_2. The main manufacturing steps included grinding of raw powders, plasticizing ground powders with a crude rubber, rolling of ceramic tapes, stacking tapes together, and hot pressing of laminates. The hot pressing conditions were as follows: a heating rate of 100 °C/min, a hot pressing temperature of 2170 °C, a pressure of 30 MPa, and a dwell time of 1 h. As a result, dense laminate samples (98–99% relative density) were obtained and further machined into $4.5 \times 5 \times 45$ mm^3 bars for four-point bending experiments. During hot pressing of the laminates, shrinkage of the individual layers occurred, and the resulting thicknesses were about 0.15 mm post-pressing. The interfaces between individual layers of the same composition completely disappeared during hot pressing. The main manufacturing steps for B_4C ceramics without rolling included grinding of raw powders and hot pressing. The hot pressing conditions were the same as previously described for the laminates.

Standard X-ray diffraction technique has been used to evaluate the phase composition of the materials and estimate if any texture appears as a result of processing steps [18].

Fracture resistance was measured by an indentation technique. Indent locations on the sample surface are shown in Fig. 1a. It follows from Fig. 1a that a top face is perpendicular to the hot pressing direction and parallel to the rolling direction, while a side face is parallel to the hot pressing direction. The indentation of surfaces was done in a way to produce cracks in planes parallel and perpendicular to the hot pressing direction. Twenty impressions have been made on the faces of the B_4C/ B_4C laminates and the B_4C ceramics without rolling. Care was taken to place the impressions far enough away from each other to ensure no interactions occurred between cracks generated from the corners of each Vickers impressions. Spatial resolution of the microhardness tester was about 1 μm, which creates an uncertainty of about 10% for the hardness value. Digital images of micrographs obtained from an optical microscope at a magnification of 100× were used for calculations. Measurement accuracy was about 0.12 μm resulting in 0.5% accuracy of measured fracture resistance and hardness values. Hardness H [GPa] was calculated using following equation

$$H = \frac{1854P}{d^2}, \tag{1}$$

where P is the indentation load (N) and d is the diagonal (μm) of a Vickers indent [19]. The fracture resistance was calculated as

$$K_R = 0.016\left(\frac{E}{H}\right)^{1/2}\frac{P}{c^{3/2}}, \tag{2}$$

where E is the Young's modulus, H is the hardness, and c is the crack length from the center of impression to the crack end [20].

Elastic modulus and strength were determined from load displacement plots that were recorded in four-point bending tests. Displacement was measured using a special three-point deflection gauge. Specimens were loaded parallel and

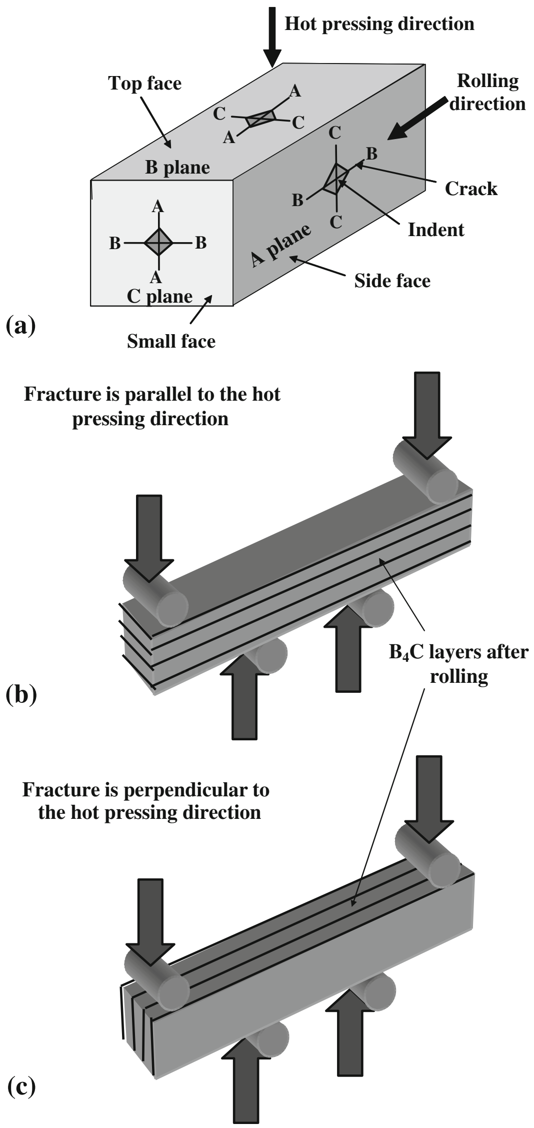

Fig. 1 A schematic presentation of the indent locations on the sample (**a**) and the sample orientation for four point bending tests (**b** and **c**)

perpendicular to the rolling plane to reveal possible differences in mechanical properties (Fig. 1b, c). The strength and elastic modulus were then determined using standard procedure EN 843-1/EN 843-2 [21, 22]. Fracture surfaces of B_4C/B_4C laminates fractured parallel and perpendicular to the hot pressing direction were investigated by scanning electron microscopy.

Results and discussion

Indentation crack length anisotropy was observed in B_4C/B_4C–30 wt%ZrB_2 laminates manufactured by rolling and hot pressing techniques. The micrograph of the Vickers impression placed in the center of thin B_4C layer is shown in Fig. 2. It is possible to see differences in the crack lengths originating from the corners of the Vickers impression, and extending in directions parallel and perpendicular to the interface. As a result, a significant difference in calculated fracture resistance values (5.8 ± 0.9 MPa $m^{1/2}$ for cracks perpendicular to the interface and parallel to the hot pressing direction, and 2 ± 0.7 MPa $m^{1/2}$ for cracks parallel to the interface and perpendicular to the hot pressing direction), using the same elastic modulus value for the calculations in both directions, is reported. Crack anisotropy can be caused by the existence of thermal residual stresses introduced during the cooling of the laminate due to the mismatch in the coefficients of thermal expansion of B_4C and B_4C–30 wt%ZrB_2 layers. However, the rolling and hot pressing can also introduce elastic anisotropy and, as result, fracture resistance anisotropy in the B_4C ceramics. These processes will also affect the crack length of the materials due to the differences in the stiffness and fracture resistance of the B_4C in different directions.

To determine what other parameters, besides thermal residual stresses, can affect the crack length of Vickers

Fig. 2 Indentation cracks on a side face of the B_4C/B_4C–ZrB_2 laminate. Note the difference in the length of Vickers cracks parallel and perpendicular to the layer interfaces

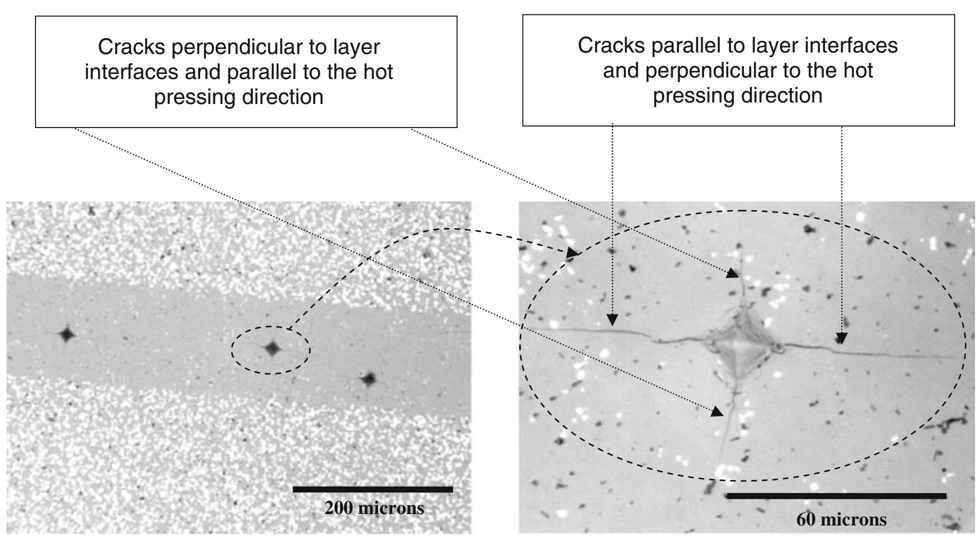

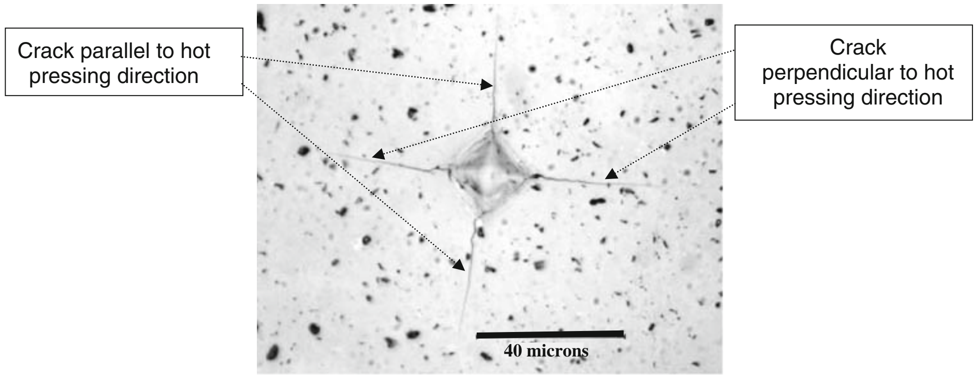

Fig. 3 Indentation cracks on the side face of rolled B_4C/B_4C laminate without compositional gradient. No difference in the crack length after indentation was noticed

impressions, indentation tests were performed on the hot pressed B_4C ceramics prepared both with and without rolling. The typical Vickers impression on the side surface of rolled B_4C/ B_4C laminate without compositional gradient is shown in Fig. 3. It is possible to see in Fig. 3 no significant anisotropy of the crack length was observed in the laminates. In other words, no thermal residual stresses were present after cooling the hot pressed sample from 2473 K to room temperature. Hardness and fracture toughness measurements performed on the three different surfaces of the hot pressed and rolled samples are summarized in Table 1. As follows from Fig. 1 and Table 1, the impression placed into the top face produced cracks in planes only parallel to the hot pressing direction, while the impression placed into the side surface generated cracks in planes parallel and perpendicular to the hot pressing direction. Therefore, there are indentation cracks on different faces produced in a parallel plane, but no significant difference in fracture resistance was detected for any of the cracks. Both fracture resistance and hardness of B_4C ceramics and B_4C/ B_4C laminate have very similar values to those reported in the literature [7, 9, 11].

The Young's modulus of B_4C/ B_4C laminates was measured using the four-point bending technique. The laminates exhibited ordinary linear deformation behavior. The laminate ceramics were loaded in two different ways. In the first case, when the fracture started from the top surface (Fig. 1b) the Young's modulus was equal to 442 ± 19 GPa (±presents the standard deviation of the measurements). In the second case when the fracture started from the side surface (Fig. 1c) the Young's modulus was equal to 486 ± 35 GPa. The strength values for both cases were 529 ± 38 MPa and 478 ± 46 MPa, respectively.

To verify that the mechanical properties do not depend on the hot pressing and rolling directions, the four-point bending tests were also performed on different B_4C–30 wt%SiC/B_4C–30 wt%SiC laminates. In the case of loading parallel to the hot pressing direction (Fig. 1b) elastic modulus was 443 ± 8 GPa and in the case of loading perpendicular to the hot pressing direction (Fig. 1c) elastic modulus was equal to 441 ± 17 GPa. The strength values for both cases were measured to be 469 ± 96 MPa and 548 ± 61 MPa, respectively.

The fractured surfaces of B_4C/B_4C laminates which fractured perpendicular and parallel to the hot pressing direction are shown in Fig. 4a and b. In both B_4C/B_4C and B_4C–30 wt%SiC/B_4C–30 wt%SiC laminates it was not possible to detect interfaces between rolled layers after hot pressing. A fully transgranular fracture mode was observed in both cases, with most of the grains retaining the equiaxial shape (Fig. 4c). The grain size was in the range of 3–6 µm. The majority of the grains had a smooth fracture surface without any cleavage. However, certain grains did

Table 1 Fracture toughness in different planes of B_4C/B_4C laminate sample

Sample	Indent location	Hardness (GPa)	Fracture toughness (MPa $m^{1/2}$)		
			Plane A (parallel to hot pressing direction)	Plane B (perpendicular to hot pressing direction)	Plane C (parallel to hot pressing direction)
Not rolled	Top face B	31 ± 2	2.6 ± 0.2		3 ± 0.4
	Side face A	31 ± 2		2.6 ± 0.3	2.7 ± 0.2
	Small face C	32 ± 2	2.5 ± 0.3	2.6 ± 0.5	
Rolled	Top face B	29 ± 1	3 ± 0.7		3.3 ± 1
	Side face A	29 ± 2		2.5 ± 0.4	2.8 ± 0.3
	Small face C	29 ± 2	2.5 ± 0.5	2.4 ± 0.3	

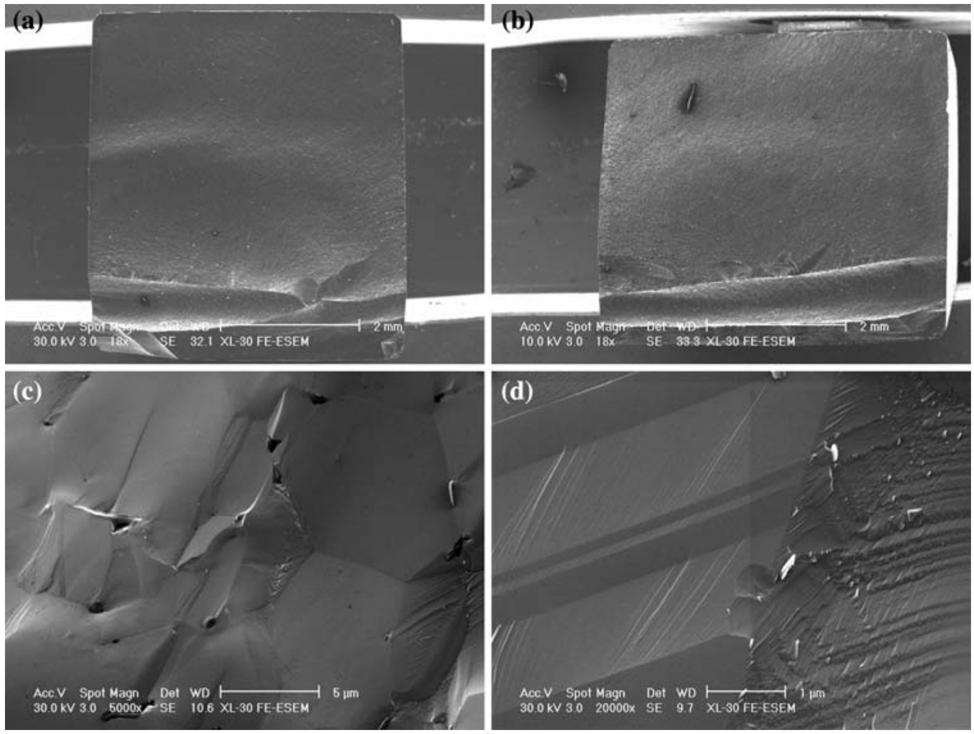

Fig. 4 Fracture surfaces of B_4C/B_4C laminates fractured parallel and perpendicular to the hot pressing direction. (**a**) a sample fractured parallel to the hot pressing direction; (**b**) a sample fractured perpendicular to the hot pressing direction; (**c**) a fracture surface of B_4C/B_4C laminates; (**d**) a fracture surface showing a twinned B_4C grain

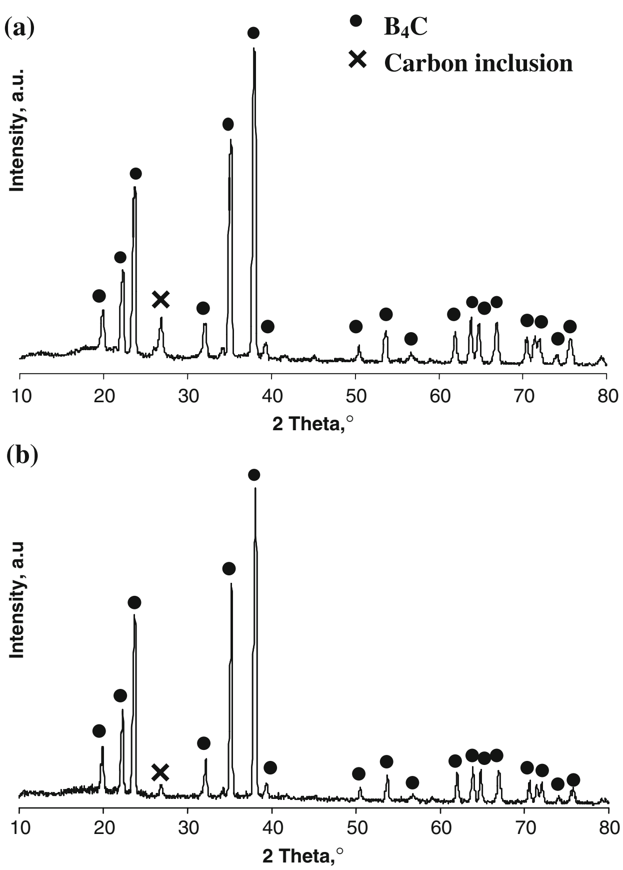

Fig. 5 XRD patterns of rolled B_4C/B_4C laminates taken from the top (**a**) and side (**b**) faces of a bending bar

exhibit cleavage steps and in some grains twinning was also detected (Fig. 4d). A small amount of intergranular porosity was present in the triple points of the grain boundary (Fig. 4c). Some insignificant amount of closed porosity within the B_4C grains has also been observed. XRD patterns of B_4C/B_4C laminates, taken from the top and side surfaces of a bending bar, are presented in Fig. 5, and they correspond to the rhombohedral B_4C structure published in other works [23, 24]. A small amount of C impurity was also detected. One can see there is no remarkable difference between the patterns, which indicates that no crystallographic texture is present in the samples. This serves as an additional evidence for the absence of anisotropy in mechanical properties [23].

Conclusions

No crack length anisotropy was found in rolled B_4C/B_4C and B_4C–30 wt%SiC/ B_4C–30 wt%SiC layered composites without a compositional gradient. Further, XRD analysis does not show crystallographic texture formation in B_4C/B_4C laminates after rolling and hot pressing. Therefore, it is possible to conclude that the Vickers crack length anisotropy in B_4C/B_4C–30 wt%ZrB_2 is a result of the thermal residual stresses originated during the cooling of the composite due to differences in the thermal expansion coefficients between the layers of the laminate.

Acknowledgements This work was supported by NSF project 0748364 "CAREER: Hard and tough boron rich ceramic laminates designed to contain thermal residual stresses," the European Commission INCO-Copernicus Grant ICA2-CT-2000-10020 "LAMINATES," Swiss Federal Office for Education and Science Grant BBW 99.0785, AFOSR, the project # F49620-02-0340, and NATO Collaborative Linkage Grant "Layered ceramic sensors for biological and chemical detection."

References

1. Johnson GR, Holmquist TJ (1999) J Appl Phys 85:8060. doi:10.1063/1.370643
2. Orphal DL, Franzen RR, Charters AC, Menna TL, Piekutowski AJ (1997) Int J Impact Eng 19:15. doi:10.1016/S0734-743X(96)00004-8
3. Chen M, Mccauley JW, Hemker KJ (2003) Science 299:1563. doi:10.1126/science.1080819
4. Bourne NK (2002) In: Proceedings of the Royal Society of London series A—mathematical, physical and engineering sciences, 458(2024), p 1999
5. Vogler TJ, Reinhart WD, Chabildas LC (2004) J Appl Phys 95:4173. doi:10.1063/1.1686902
6. Niihara K, Nakahira A, Hirai T (1984) J Am Ceram Soc 67:13
7. Champagne B, Angers R (1979) J Am Ceram Soc 62:149. doi:10.1111/j.1151-2916.1979.tb19042.x
8. Yamada S, Sakaguchi S, Hirao K, Yamauchi Y, Kanzaki S (2003) J Ceram Soc Jpn 111:53. doi:10.2109/jcersj.111.53
9. Thevenot F (1990) J Eur Ceram Soc 6:205. doi:10.1016/0955-2219(90)90048-K
10. Abzianidze TG, Eristavi AM, Shalamberidze SO (2000) J Solid State Chem 154:191. doi:10.1006/jssc.2000.8834
11. Lee H, Speyer R (2002) J Am Ceram Soc 85:1291
12. Orlovskaya N, Lugovy M, Ko F, Yarmolenko S, Sankar J, Kuebler J (2006) Compos B 37:524. doi:10.1016/j.compositesb.2006.02.022
13. Orlovskaya N, Lugovy M, Kuebler J, Mechanical performance of 3 layered B_4C/B_4C-SiC laminates (in preparation)
14. Tariolle S, Reynaud C, Thevenot F, Chartier T, Besso JL (2004) J Solid State Chem 177:487. doi:10.1016/j.jssc.2003.02.007
15. Mcclellan KJ, Chu F, Roper JM, Shindo I (2001) J Math Sci 36:3403. doi:10.1023/A:1017947625784
16. Radchenko A, Subbotin V, Lugovy M, Orlovskaya N, Fracture toughness anisotropy of hot pressed silicon nitride (in preparation)
17. Orlovskaya N, Lugovy M, Subbotin V, Radchenko O, Adams J, Cheda M et al (2005) J Math Sci 40:5483. doi:10.1007/s10853-005-1923-x
18. Kakazey M, Vlasova M, Gonzalez-Rodriguez JG, Dominguez-Patino M, Leder R (2006) Mater Sci Eng A 418:111. doi:10.1016/j.msea.2005.11.018
19. Tabor D (1951) Hardness of metals. Clarendon Press, Oxford
20. Antis GR, Chantikol P, Lawn BR, Marshall DB (1981) J Am Ceram Soc 64:533. doi:10.1111/j.1151-2916.1981.tb10320.x
21. European Standard EN 843-1, Advanced technical ceramics—Mechanical properties of monolithic ceramics at room temperature—Part 1: determination of flexural strength, December 2006
22. European Standard EN 843-2, Advanced technical ceramics—Mechanical properties of monolithic ceramics at room temperature—Part 2: determination Young's modulus, shear strength and Poisson's ratio, December 2006
23. Anselmi-Tamburini U, Ohyanagi M, Munir ZA (2004) Chem Mater 16:4347. doi:10.1021/cm049195q
24. Lemis-Petropoulos P, Kapaklis V, Peikrishvili AB, Politis C (2003) J Mod Phys B 17:2781. doi:10.1142/S0217979203018582